Charge density waves in *B*2 compounds of titanium

I. I. Naumov, O. I. Velikokhatnyĭ, and V. Z. Bashirov
Institute of the Physics of Strength and Materials Science, 634048, Tomsk

(Submitted 11 October 1991)
Pis'ma Zh. Eksp. Teor. Fiz. **54**, No. 10, 571–574 (25 November 1991)

A first-principles calculation of the electronic structure shows that states with charge density waves can arise not only in TiNi but also in other *B* 2 compounds of titanium: TiPd and TiPt. In addition, the set of such states in this class of compounds may be richer than the set which TiNi has previously been believed to have.

It has recently been established[1,2] that when the *B* 2 compound TiNi is cooled it becomes unstable with respect to the formation of charge density waves. The formation of these waves is accompanied by a phase transition from the original *B* 2 (CsCl) structure into an incommensurate (*IC*) phase, characterized by extra diffractive-scattering reflections in slightly incommensurate positions of the types $\mathbf{q}_{\rm I} \approx (2/3)\langle 110\rangle$ and $\mathbf{q}_{\rm II} \approx (2/3)\langle 111\rangle$ (in units of π/a, where a is the side of the unit cube).[1,3] The formation of the charge density waves or the occurrence of the $B\,2 \rightarrow IC$ transition is preceded by a softening of the transverse acoustic vibrational branch Σ_4 at $\mathbf{q} \approx \mathbf{q}_{\rm I}$. Compensation then occurs right at the transition point.[4,5] Upon further cooling, the *IC* phase undergoes a transition into a commensurate *R* phase: On the average, the cubic *IC* structure acquires a rhombohedral distortion, as a result of which some of the split Bragg reflections become comparable to vectors of the types[1,3] $\mathbf{q}_I$ and $\mathbf{q}_{II}$.

Numerical first-principles calculations[6] of the electronic structure by a strong-coupling method have shown that a phonon instability and the formation of charge density waves in TiNi can be linked with geometric features of the Fermi surface. Regions of the electron Fermi surface (zone 8) and of the hole Fermi surface (zone 7) which have the same shape were observed. These regions lead to a sharp peak in the generalized susceptibility $\chi(\mathbf{q},0)$ and, correspondingly, to a dip in the Σ_4 phonon branch at $\mathbf{q} = \mathbf{q}_{\rm I}$.

Zhao *et al.*[6] believe that the nesting between sheets 7 and 8 of the Fermi surface in TiNi is simply fortuitous and that the structural instability which they discussed is unique. In the present letter we show that, on the contrary, isoelectronic analogs of TiNi–TiPt and TiPd—also tend to undergo an instability of this type, although in TiPd (for example) the topology of the Fermi surface is not the same as that in TiNi. Moreover, the electronic structure of this class of *B* 2 compounds is such that under favorable conditions charge density waves and incommensurate structures, characterized by wave vectors differing from $\mathbf{q}_{\rm I}$ and $\mathbf{q}_{\rm II}$, can also form in them.

The electronic structure and the generalized susceptibility of the noninteracting electrons,

$$\chi(\mathbf{q},0) = \frac{2\Omega}{(2\pi)^3} \int dk \sum_{n,n'} \frac{f(\epsilon_n(\mathbf{k}))[1 - f(\epsilon_{n'}(\mathbf{k}+\mathbf{q}+\mathbf{g}))]}{\epsilon_{n'}(\mathbf{k}+\mathbf{q}+\mathbf{g}) - \epsilon_n(\mathbf{k})}, \tag{1}$$

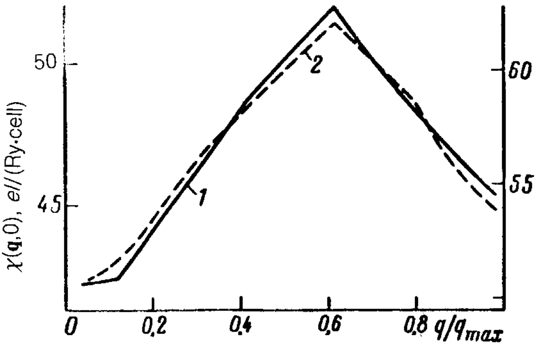

FIG. 1. Generalized susceptibility $\chi(\mathbf{q},0)$ in the ⟨100⟩ direction. 1—TiPt, scale at left; 2—TiPd, scale at right.

which were required for the analysis, were calculated by the LMTO method, with allowance for combined corrections.[7] In the integration over k in (1) we used the highly accurate tetrahedron method.[8] The irreducible part (1/48) of the Brillouin zone was partitioned into 1728 microtetrahedra. We took only zones 7 and 8, which intersect the Fermi level, into account. In other words, we took account of only the transitions 7→7, 7→8, 8→7, and 8→8 [the other transitions make only noncritical contributions to $\chi(\mathbf{q},0)$].

Figure 1 shows $\chi(\mathbf{q},0)$ for TiPt and TiPd along the ⟨110⟩ direction. We see that the functions $\chi(\mathbf{q},0)$ have sharp peaks at essentially the same vector, $\mathbf{q}_n = 0.61\langle 110\rangle$, which is close to $\mathbf{q}_{\mathrm{I}}$. Analysis of the partial contributions shows that these peaks stem from 8→7 electronic transitions.

To determine the nature of these peaks, we examine the Fermi surface. In TiPt, as in TiNi (Ref. 6), this surface has two closed electron pockets, which are centered at

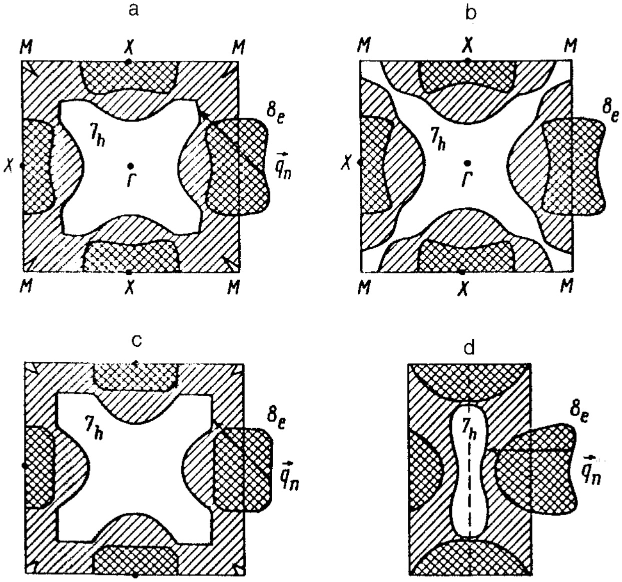

FIG. 2. Cross sections of the Fermi surface. a—TiPd, $k_z = 0$; b—TiPd, $k_z = 0$; c—TiPd, $k_z = \pm 0.1$; d—TiPd, plane parallel to (110) containing the nesting vector $\mathbf{q}_n$.

the X and R points ($8X_e$,$8R_e$), and two closed hole pockets, which surround the Γ and M points ($7\Gamma_h$,$7M_h$). Here 7 and 8 are the indices of the corresponding energy bands. The $7\Gamma_h$ and $7M_h$ hole pockets, which are stretched out toward each other, exhibit a tendency to form a bridge (Fig. 2a). A bridge of this sort also forms in TiPd, and as a result the hole Fermi surface (7_h) in that system becomes open with respect to ΓM or $\langle 110\rangle$ directions (Fig. 2b). The nesting vector $\mathbf{q}_n$ for TiPt is shown in Fig. 2a, in the plane with $k_z = 0$. This section, however, does a poor job of reflecting the scale of the nesting, which extends above and below the given plane to $k_z = \pm 0.2$. In the case of TiPd, in the plane with $k_z = 0$, it is totally impossible to find a vector $\mathbf{q}_n$ which would connect sheets of the Fermi surface with identical curvature. This circumstance is evidently a consequence of the formation of a bridge. The intersections of the Fermi surface in the planes with $k_z = \pm 0.1$ and in the perpendicular plane, which contains the nesting vector $\mathbf{q}_n$ (Fig. 2, c and d), give an idea of the scale of the nesting in this compound (as in TiNi and TiPt).

In addition to the nesting, there is another factor which makes the $\chi(\mathbf{q},0)$ peak at $\mathbf{q} \approx \mathbf{q}_{\mathrm{I}}$ stable and clearly expressed in these compounds. To explain the situation, we consider Eq. (1) with $n = 8$ and $n' = 7$, without the denominator. In this case, Eq. (1) simply gives the phase volume for $8 \to 7$ transitions. Taking into account the $8 \to 7$ transitions from the $8X_e$ pocket alone (not from $8R_e$) for the moment, we displace this pocket along the $\langle 110\rangle$ axis with respect to the 7_h surface (Fig. 2, a and b). At $\mathbf{q} = 0$, no allowed $8 \to 7$ transitions are allowed, and the contribution to the volume corresponding to these transitions, $\chi(\mathbf{q},0)$, is zero (the $8X_e$ and 7_h surfaces do not intersect). Beginning at $\mathbf{q} = \mathbf{Q}_{\mathrm{I}}$, which corresponds to the tangency of these surfaces, transitions of this sort appear, and $\chi(\mathbf{q},0)$ increases along with $\mathbf{q}$, in an approximately linear fashion. Later, $\chi(\mathbf{q},0)$ unavoidably goes through a maximum, since at $\mathbf{q} = \mathbf{Q}_{\mathrm{II}} > \mathbf{Q}_{\mathrm{I}}$ the intersection of the $8X_e$ and 7_h surfaces disappears again, and the phase volume must vanish. Numerical calculations for TiPd show that the phase volume reaches a maximum at $\mathbf{q} \approx 0.5\langle 110\rangle$.

The phase volume behaves in this manner when the $8 \to 7$ transitions from the $8R_e$ pocket alone are taken into account: We find $\chi(\mathbf{q},0) = 0$ at $\mathbf{q} = 0$; then there is a nearly linear increase with $\mathbf{q}$. Thereafter, $\chi(\mathbf{q},0)$ goes through a maximum, but remains finite at "large" $\mathbf{q}$ all the way to the boundary of the Brillouin zone. Numerical calculations for TiPd lead to a maximum in $\chi(\mathbf{q},0)$ at $\mathbf{q} \approx 0.7\langle 110\rangle$ in this case. When the $8 \to 7$ transitions from the $8X_e$ and $8R_e$ pockets are taken into account simultaneously, the maximum occurs at $\mathbf{q} \approx \mathbf{q}_n \approx \mathbf{q}_{\mathrm{I}}$! The role of nesting [which is reflected in the denominator in (1)] now reduces to cresting this peak.

It is not difficult to see that the "phase-volume effect" which we have just looked at could also promote the appearance of maxima in $\chi(\mathbf{q},0)$ at wave vectors other than $\mathbf{q}_{\mathrm{I}}$ (as in the case $\mathbf{q} = \mathbf{q}_{\mathrm{I}}$, the maxima can be fairly sharp if nesting effects are also operating). Calculations for TiNi show that vectors in this category are $\mathbf{q}_{\mathrm{III}} \approx 2/3,\langle 1,1/2,0\rangle$, $\mathbf{q}_{\mathrm{IV}} \approx 2/3\langle 1,2/3,1/3\rangle$ (Fig. 3), $\mathbf{q}_{\mathrm{V}} \approx 2/3\langle 1,1/2,1/2\rangle$, etc.

The peaks in $\chi(\mathbf{q},0)$ at $\mathbf{q} \approx \mathbf{q}_{\mathrm{I}}$ in TiPt and TiPd suggest that charge density waves may form in these compounds, like the ones which form in TiNi. The experimental evidence presently available indicates that there are no charge density waves in these materials when they have their stoichiometric compositions. However, even a small

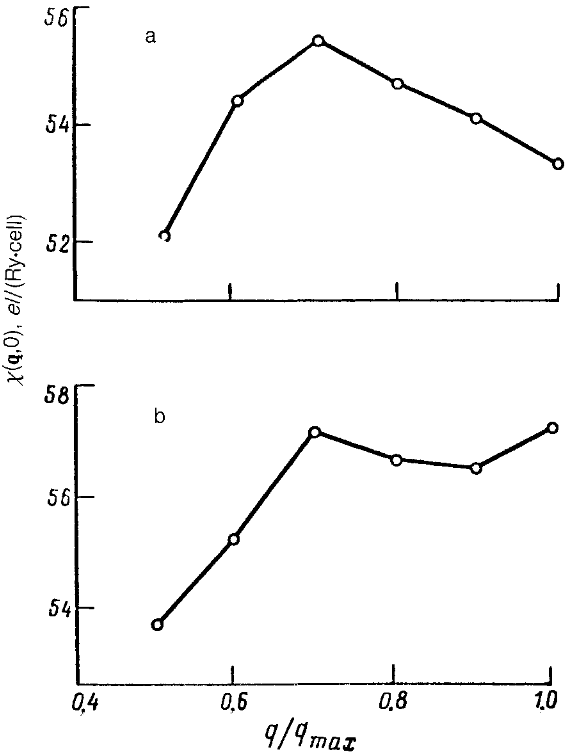

FIG. 3. Generalized susceptibility $\chi(\mathbf{q},0)$ in TiNi. a—⟨1,1/2,0⟩; b—⟨1,2/3,1/3⟩.

admixture of Fe (~5%) in TiPd gives rise to an incommensurate phase in this sytem. This phase is very similar to that which occurs in TiNi (Ref. 9). It also gives rise to a 9*R* phase, which Enami *et al.*[9] believe plays the role of a commensurate phase in a lock-in transition: commensurate→9*R*. Enami *et al.*[9] stress that the *IC* phase in TiPd-based alloys is characterized by structural reflections which are more incommensurate than those in TiNi. That interpretation agrees with our own calculations: The $\chi(\mathbf{q},0)$ peak in TiNi corresponds to $\mathbf{q} = 0.66\langle 110\rangle$, which is closer to $(2/3)\langle 110]$ than the $0.61\langle 110\rangle$ in the case of TiPd.

Our results also suggest the possible formation of charge density waves in TiNi, TiPt, and TiPd with wave vectors different from $\mathbf{q}_{\mathrm{I}}$. Significant in this connection is the circumstance that a so-called *R* ′ phase, which forms in parallel with the *R* phase, which we have already mentioned, was recently observed[10] in TiNi. The *R* ′ phase is characterized by extra reflections in $\mathbf{q}_{\mathrm{III}}$ and $\mathbf{q}_{\mathrm{IV}}$ positions which (as we have already mentioned) give rise to maxima in the function $\chi(\mathbf{q},0)$. Zhao *et al.*[10] suggest that, like the *R* phase, the *R* ′ phase can be thought of as the product of a lock-in transition from some state with charge density waves. Our own data agree with that suggestion.

In summary, this analysis shows that charge density waves can be assumed to occur not exclusively in TiNi but also in other *B* 2 compounds of titanium. The picture of states with charge density waves in these compounds may be considerably richer than that which has previously been assumed for TiNi. Further experiments will be required to test these conclusions.

We deeply thank V. G. Vaks, A. V. Trefilov, and I. I. Mazin for discussion of these results. We also thank V. N. Khachin for support of this work.

[1] M. B. Salamon, M. E. Meichle, and C. M. Wayman, Phys. Rev. B **31**, 7306 (1985).
[2] S. A. Shabalovskaya, Phys. Status Solidi B **132**, 327 (1985).
[3] I. Folkins and M. B. Walker, Phys. Rev. B **40**, 255 (1989).
[4] G. Herget, M. Mullner, G. Eckold, and H. Jex, *Proceedings of the Third Conference on Phonon Physics and Sixth International Conference in Condensed Matter,* Heidelberg, 1989, pp. 55–57.
[5] H. Tietze, M. Mullner, and B. Renker, J. Phys. C **17**, L529 (1984).
[6] G.-L. Zhao, T. C. Leung, B. N. Harmon *et al.*, Phys. Rev. B **40**, 7999 (1989).
[7] O. K. Andersen, Phys. Rev. B **12**, 3060 (1975).
[8] J. Rath and A. J. Freeman, Phys. Rev. B **11**, 2109 (1975).
[9] K. Enami, T. Yoshida, and S. Nerno, *Proceedings of the International Conference on Martensitic Transformations* (ICOMAT-86), Nara, 1986, pp. 103–108.
[10] X. Zhao, X. Wu, and T. Ko, Acta Metall. **37**, 1783 (1989).

Translated by D. Parsons